Species' ranges and the steepening-gradient hypothesis

Matteo Tomasini[1,2,*], Martin Eriksson[1,2,3], Kerstin Johannesson[2,4], and Marina Rafajlović[1,2,*]

[1]Department of Marine Sciences, University of Gothenburg, SE-40530, Gothenburg, Sweden

[2]Centre for Marine Evolutionary Biology, University of Gothenburg, SE-40530, Gothenburg, Sweden

[3]Gothenburg Global Biodiversity Centre, University of Gothenburg, SE-40530, Gothenburg, Sweden

[4]Department of Marine Sciences, University of Gothenburg, SE-45296, Strömstad-Tjärnö, Sweden

[*]Corresponding authors: matteo.tomasini@gu.se, marina.rafajlovic@marine.gu.se

March 19, 2022

Abstract

One hypothesis invoked to explain limits to species' ranges is a mismatch in environmental conditions between the central and marginal areas of species' ranges. Low population size at the margins causes genetic drift to outplay selection locally, and limits the accumulation of genetic variance, so that adaptation is hindered locally. Earlier theoretical work shows that for a population expanding over a spatially heterogeneous environment without any geographical barriers, adaptation will fail abruptly, which establishes definite range margins only when the underlying environmental conditions change more and more severely across space, whereas an environment changing constantly results either in infinite expansion or rapid global extinction. Here, we extend the steepening-gradient hypothesis to encompass situations when environmental gradients are decomposed into selection acting on separate adaptive traits. We show that the two gradients steepen each other, particularly highlighting the importance of locally shallow gradients that could be overlooked in field studies. Finally, by decomposing the environmental gradient to selection on two adaptive traits, populations can withstand harsher environmental conditions than when selection acts on one adaptive traits alone.

Introduction

Populations' range margins can form due to discontinuities in the environment, such as geographical barriers (*e.g.* mountain ranges, rivers) [Holt, 2003]. However, sometimes range margins seem to occur abruptly along smooth environmental gradients, in the absence of any obvious geographical barriers [Bridle and Vines, 2007]. A question that has puzzled ecologists and evolutionary biologists for a long time,

is whether range margins can arise solely as a result of a failure to adapt along spatially changing environmental conditions [Mayr, 1963, MacArthur, 1963], or if a concomitant cause is needed, such as species competition [Case et al., 2005, Bridle and Vines, 2007], or reducing carrying capacity [Gomulkiewicz et al., 1999].

A potential mechanism leading to the formation of sharp range margins is asymmetric gene flow from more densely populated parts of the habitat (*e.g.* centre) swamping locally beneficial alleles at the margins [Haldane, 1956, Mayr, 1963, Kirkpatrick and Barton, 1997, Peck et al., 1998, Barton, 2001]. However, it has been shown that asymmetric gene flow alone is insufficient to generate range margins. For example, when the optimal phenotype of the adaptive trait changes linearly in space, a population can expand indefinitely (or up to the habitat boundaries), unless the gradient in the optimum is too steep, in which case the population will face rapid global extinction [Barton, 2001]. Global extinction along steep gradients occurs because gene flow generates too much genetic variance (*i.e.* genetic load), which, in turn, reduces the local population size to the point where drift overpowers selection, causing adaptation to fail everywhere [Polechová and Barton, 2015]. Conversely, if the gradient in the optimal phenotype steepens in space, adaptation will fail when the local steepness of the gradient reaches the point where too much genetic variance is needed to maintain the population at the optimum, leading to the formation of a sharp range margin [Polechová and Barton, 2015, Polechová, 2018]. This finding puts forward a "steepening-gradient hypothesis" for species' range limits: the steepening-gradient hypothesis states that, in the absence of geographic barriers or competitors, range margins can form where the gradient in the optimal phenotype steepens sufficiently in space.

So far, the theoretical treatment of the steepening-gradient hypothesis has taken into account the evolution of a single adaptive trait. However, empirical studies have provided evidence that, in natural populations, multiple adaptive traits are likely involved (*e.g.* Manel and Holderegger [2013], Dayan [2020]). Here we expand the steepening-gradient hypothesis put forward by Polechová and Barton [2015] in two directions. First, we assess how the formation of range margins is impacted by the interplay between two adaptive traits, one with the gradient in the optimal phenotype that steepens in space, and one with a linear optimal phenotype. By imposing two components of selection, a lower population fitness is expected compared to when only one of the selection components (acting on a single trait) is involved [Barton, 2001]. However, because a population is expected to expand indefinitely over a linearly changing optimum, it is unclear if, and how, added selection in the form of a linearly changing optimal phenotype affects the realised range of a population. Second, we ask how range expansion in a situation with one adaptive trait with a given optimal phenotype compares to expansion in a situation where this optimal phenotype is decomposed between two adaptive traits, one with a steepening and one with a constant gradient in the optimal phenotype.

We show that individual selection gradients steepen each other, leading to smaller ranges than when any individual gradient acts alone. Notably, this is true even when one gradient is very shallow, such that it can be overlooked in field studies. Furthermore, we show that a population attains a larger range when the selection gradient is decomposed into two (or more) orthogonal adaptive traits than when it acts on a single adaptive trait. This is because with two adaptive traits, the covariance between the phenotypes of the traits reduces the individuals' fitness cost due to a mismatch between their phenotypes and the local optimum, compared to the single trait model.

Results

Model summary

Similarly to Eriksson and Rafajlović [2021, 2022], we modelled a monoecious population with non-overlapping generations expanding from the central region of a unidimensional habitat composed of 180 demes, each with the carrying capacity of $K = 100$ individuals. At the beginning of the simulations, the central region of 36 demes was filled with locally well adapted populations (Methods). At each generation τ, the fitness of individual l in deme $i \in \{1, 2, \ldots, 180\}$ was determined by the local population size $N_\tau^{(i)}$, and by the individual's phenotype $z_{\tau,l}^{(j,i)}$ of two polygenic adaptive traits ($j \in \{1, 2\}$) with respect to their optimal phenotypes $\theta^{(j,i)}$. Each adaptive trait was underlain by a separate set of L freely recombining biallelic loci. Alleles were assumed to contribute additively to the phenotype with $\pm\alpha/2$. The two traits were assumed to have spatially heterogeneous optimal phenotypes $\theta^{(j,i)}$, such that $\theta^{(1,i)}$ had a steepening gradient in space (eq. S1) and $\theta^{(2,i)}$ was linear in space (eq. S2). We assumed that the two traits were orthogonal, *i.e.* that if the trait value of one of the two traits was the same in two individuals in the same deme, then the difference in fitness of these individuals would be determined by the other trait only. The growth rate of each individual was

$$r_{\tau,l}^{(i)} = r_{\max}\left(1 - \frac{N_\tau^{(i)}}{K}\right) - \frac{\left(z_{\tau,l}^{(1,i)} - \theta^{(1,i)}\right)^2}{2V_s} - \frac{\left(z_{\tau,l}^{(2,i)} - \theta^{(2,i)}\right)^2}{2V_s}\,, \tag{1}$$

where $r_{\max}$ is the maximal intrinsic growth rate of the population ($r_{\max} = 1$ throughout). The second and the third term are the contributions due to selection acting on the first and second trait, respectively, in line with Fisher's geometric model involving two orthogonal traits [Fisher, 1930]. Here, V_s is the width of stabilizing selection, and we set it to the same value for both traits for simplicity.

To understand how an additional selection component in the form of a constant gradient may modify the establishment of range margins, we first compared this model with two adaptive traits to the model involving only one adaptive trait with the steepening gradient in $\theta^{(1,i)}$ (upon letting $V_s \to \infty$ for the second trait, making it a neutrally evolving trait). Thereafter, we aimed at understanding if a population is more or less successful in expanding its range when a composite environmental gradient is decomposed into environmental selection acting on two traits as opposed to it acting on one trait only. To achieve this, we compared our two-trait model with a model where the phenotype was $z_{\tau,l}^{(c,i)} = z_{\tau,l}^{(1,i)} + z_{\tau,l}^{(2,i)}$, the composite optimal phenotype was $\theta^{(c,i)} = \theta^{(1,i)} + \theta^{(2,i)}$, and the growth rate $r_{\tau,l}^{(c,i)}$ for individual l in deme i at generation τ in the composite single-trait model was:

$$r_{\tau,l}^{(c,i)} = r_{\max}\left(1 - \frac{N_\tau^{(i)}}{K}\right) - \frac{\left((z_{\tau,l}^{(1,i)} + z_{\tau,l}^{(2,i)}) - (\theta^{(1,i)} + \theta^{(2,i)})\right)^2}{2V_s}\,. \tag{2}$$

Because in this model the two sets of loci contribute to the same composite phenotype, we call this the "composite single-trait model", or just "single-trait model".

Throughout, quantities without the subscript τ are quantities at the end of simulations (*i.e.* quasi-equilibrium, albeit, like others, *e.g.* Barton [2001], and for simplicity, we refer to this state as equilibrium).

At each generation, after selection, recombination, mutation and fertilization took place, individuals dispersed following a discretised Gaussian distribution centered around their native deme and with standard

deviation of $\sigma = 1$ [Eriksson and Rafajlović, 2021]. Simulations were run for 100,000 generations, with 50 independent replicates per parameter set.

We explored 4 different values of the steepness $b^{(2)}$ of the linearly changing optimal phenotype $\theta^{(2,i)}$, while keeping $b^{(1,i)} = \partial\theta^{(1,d)}/\partial d|_{d=i}$ the same in each case (Methods; table 1). At the end of each simulation, before migration took place in the last simulated generation, we measured the range attained, the local population size $N^{(i)}$ along the range, as well as the genetic variance $v^{(j,i)}$ for each trait. We also used the theoretical expectations (population size, genetic variance) for the single-trait steepening-gradient model as a baseline for comparisons [Polechová and Barton, 2015].

Notation	Description
M	number of demes, $M = 180$
K	carrying capacity per deme, $K = 100$
$N_\tau^{(i)}$	local population size in deme i at generation τ
$z_{\tau,l}^{(j,i)}$	phenotype for trait j of individual l in deme i at generation τ
$z_{\tau,l}^{(c,i)} = z_{\tau,l}^{(1,i)} + z_{\tau,l}^{(2,i)}$	composite (single) phenotype of individual l in deme i at generation τ
$\theta^{(j,i)}$	optimal phenotype of trait j in deme i (Appendix A, eq. (S1) and eq. (S2))
$\theta^{(c,i)} = \theta^{(1,i)} + \theta^{(2,i)}$	composite (single) optimal phenotype in deme i
$r_{\tau,l}^{(i)}$	growth rate of individual l in deme i at generation τ in the two-trait model
$r_{\tau,l}^{(c,i)}$	growth rate of individual l in deme i at generation τ in the single-trait model
$b^{(1,i)}$	local steepness of the optimal phenotype with steepening gradient in deme i (*i.e.* $b^{(1,i)} = \partial\theta_{1,d}/\partial d|_{d=i}$)
$b^{(2)}$	steepness of the linear optimal phenotype, $b^{(2)} \in \{0, 0.5, 1, 1.5\}$
$b^{(c,i)} = b^{(1,i)} + b(2)$	local steepness of the composite (single) optimal phenotype in deme i
$v_\tau^{(1,i)}$	genetic variance for trait 1
$v_\tau^{(2)}$	genetic variance for trait 2
L	number of loci underlying each trait, $L = 654$
$\pm\alpha/2$	allelic effect size, $\alpha = 1/\sqrt{10}$
V_s	width of selection, $V_s = 2$
$r_{\max}$	maximal intrinsic growth rate, $r_{\max} = 1$
μ	mutation rate, $\mu = 10^{-6}$
σ	standard deviation of dispersal (discretised Gaussian dispersal), $\sigma = 1$

Table 1: Notations used in the main text. For further details on model implementation and parameters, see Methods.

Failure to adapt and reduced range

The genetic variance for the trait with the steepening gradient in optimal phenotype (hereafter trait 1) follows the expected genetic variance for a population expanding over the steepening gradient alone, *i.e.* $v^{(1,i)} = b^{(1,i)}\sigma\sqrt{V_s}$ (blue dashed line in figure 1A) [Barton, 2001, Polechová and Barton, 2015]. The genetic variance for the trait with the optimal phenotype that changes linearly across the habitat (hereafter trait 2) is approximately constant across the realised range, in line with theory for a single-trait model [Barton, 2001]. However, the expected genetic variance for a population expanding over the constant gradient $\theta^{(2,i)}$, *i.e.* $v^{(2,i)} = b^{(2)}\sigma\sqrt{V_s}$, is higher than the value realised in simulations when the variance is measured before migration (compare dashed and solid lines in figure 1B). By contrast, when genetic variance is measured after migration, linkage disequilibrium inflates variance (fig. S9, Appendix C) to the point where variance is higher than expected in the deterministic model [Barton, 2001]. In either case, the difference between the expected and realised genetic variance was larger for larger values of $b^{(2)}$. This was not due to the interplay between traits, but rather to the linkage disequilibrium inflating genetic variance more for steeper gradients and stronger drift (Appendix D). The spatial pattern of the variance for trait 2 is retained for all values of $b^{(2)}$ employed here, *i.e.* we find that the variance $v^{(2,i)}$

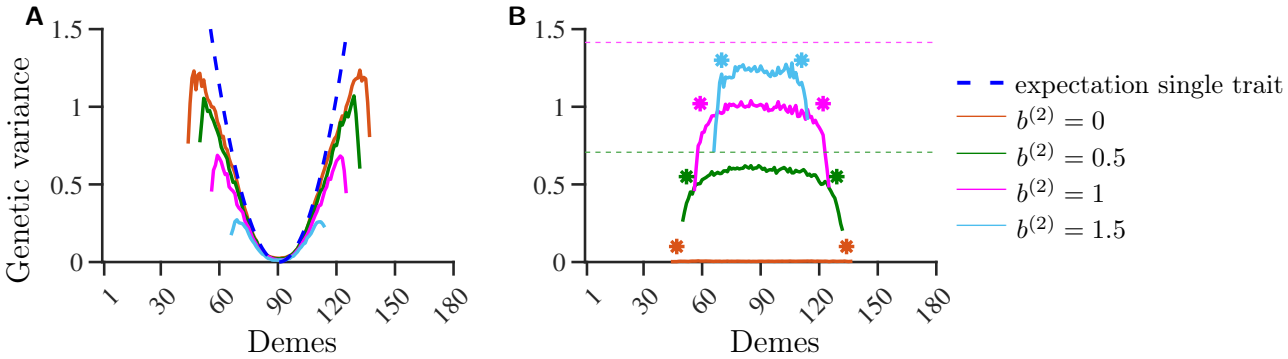

Figure 1: Genetic variance averaged over 50 independent realisations for each different value of the steepness of the constant gradient, $b^{(2)}$, for the phenotype of trait 1 (A) or trait 2 (B), as a function of deme position. The dashed blue line corresponds to the expected genetic variance with just the steepening gradient. The solid lines correspond to the two-trait model with $b^{(2)} = 0$ (orange), $b^{(2)} = 0.5$ (green), $b^{(2)} = 1$ (magenta), and $b^{(2)} = 1.5$ (cyan). In (A) the blue dashed line shows the expected variance for trait 1 for a single-trait model, *i.e.* $v^{(1,i)} = b^{(1,i)}\sigma\sqrt{V_s}$. In (B), green and magenta dashed lines represent the expected variance for trait 2, $v^{(2,i)} = b^{(2)}\sigma\sqrt{V_s}$ (colored according to the figure legend). The y-axis is truncated at 1.5 for clarity; therefore, the expected genetic variance for $b^{(2)} = 1.5$ (*i.e.* $v^{(2,i)} \approx 2.12$) is not shown. The stars denote where adaptation fails according to maximum variance in (A) (colored according to the figure legend). Other parameters: $\alpha = 1/\sqrt{10}$, $V_s = 2$, $\sigma = 1$, $r_{\max} = 1$, $L = 654$, $K = 100$, and $\theta^{(1,i)}$, $\theta^{(2,i)}$ as given in Appendix A, (S1) and (S2) respectively.

is approximately spatially constant, although it is slightly concave due to the lower population size near the margins.

We found that the realised range is smaller when $b^{(2)}$ is larger (fig. 1; recall that $b^{(1,i)}$ was fixed). In other words, the two gradients steepen each other. Notably, we find that, at the margins, the steepening gradient is shallower when the second, constant, gradient ($b^{(2)}$) is larger. Recall that a constant gradient by itself cannot cause the formation of non-trivial range margins (*sensu* Eriksson and Rafajlović [2022]). But when a steepening gradient, despite being almost flat, is added on top of a constant gradient, a non-trivial range margin is readily formed (fig. 2).

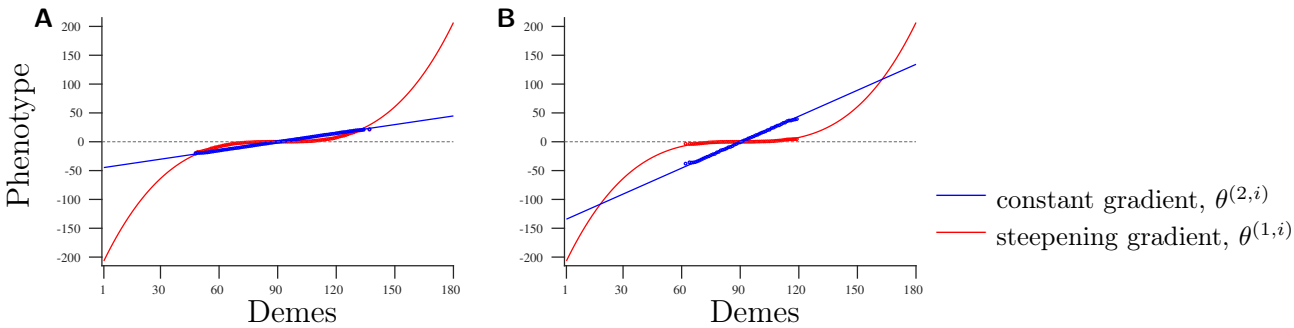

Figure 2: Optimal phenotypes $\theta^{(1,i)}$ (steepening gradient; red line) and $\theta^{(2,i)}$ (constant gradient; blue line). Further details on the gradients are given in Appendix A. The thicker line shows realised local mean phenotypes at the end of simulations, averaged over 50 independent realisations of range expansion. The constant gradient $b^{(2)}$ was $b^{(2)} = 0.5$ (A), or $b^{(2)} = 1.5$ (B) (scenarios with $b^{(2)} = 0$ and $b^{(2)} = 1$ are not shown). Other parameters: $\alpha = 1/\sqrt{10}$, $V_s = 2$, $\sigma = 1$, $r_{\max} = 1$, $L = 654$, $K = 100$.

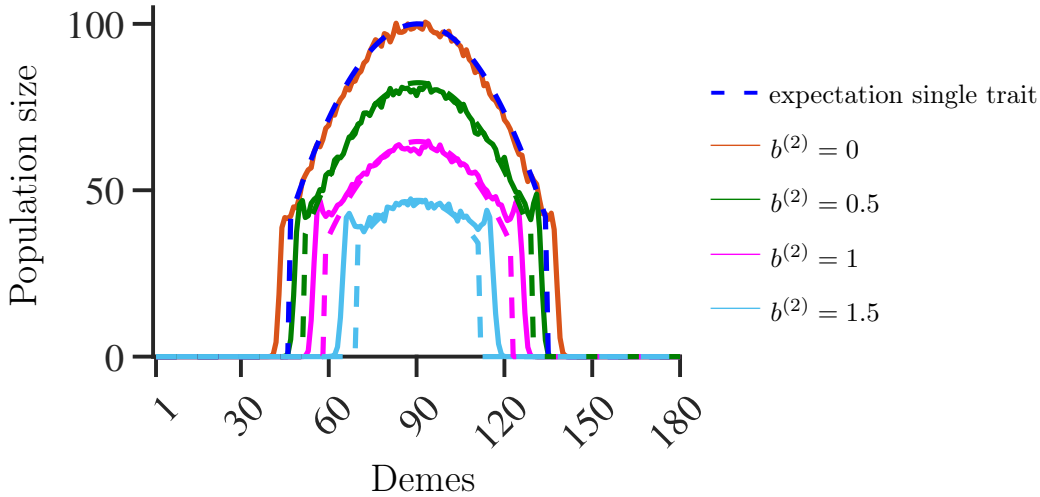

Figure 3: Population size averaged over 50 independent realisations for different values of the steepness of the constant gradient, $b^{(2)}$, as a function of deme position. Solid lines show realised population size at the end of simulations for $b^{(2)} = 0$ (orange), $b^{(2)} = 0.5$ (green), $b^{(2)} = 1$ (magenta), and $b^{(2)} = 1.5$ (cyan). Blue dashed line shows the expected population size with only the steepening gradient $b^{(1,i)}$, *i.e.* $N^{(i)} = K(1 - b^{(1,i)}\sigma/(2\sqrt{V_s}r_{\max})$, truncated at the realised range margins. Green, magenta and cyan dashed lines show our analytical approximation for the population size accounting for the sum of adaptive genetic variances as in (3), truncated at the realised range margins. Other parameters: $\alpha = 1/\sqrt{10}$, $V_s = 2$, $\sigma = 1$, $r_{\max} = 1$, $L = 654$, $K = 100$, and $b^{(1)}$ as defined in Appendix A (equation (S1)).

The sum of adaptive genetic variances determines the population size

Recall that when $b^{(2)}$ is larger, a population attains a smaller range. In addition, a larger $b^{(2)}$ causes the population size to be smaller in each deme, suggesting that the population is more maladapted along the habitat, because the genetic load is larger when $b^{(2)}$ is larger (fig. 1). In the special case when the optimal phenotype $\theta^{(2,i)}$ is spatially constant ($b^{(2)} = 0$, orange line in figure 3), the realised range and the population size are the same as in the case with the steepening gradient $\theta^{(1,i)}$ only (blue dashed line, fig. 3).

In our two-trait model, we found that the population size around the center follows the expectation given by (for a single-trait model) Polechová and Barton [2015], but with the genetic variance determined by the sum of expected genetic variances for traits 1 and 2 ($v^{(1,i)} + v^{(2)}$):

$$N^{(i)} = K\left(1 - \frac{v^{(1,i)} + v^{(2)}}{2V_s r_{\max}}\right), \tag{3}$$

As expected, the population size decreases from the center to the margins. Interestingly, however, we observe that the population size shows a slight increase in the vicinity of the range margins, before it abruptly drops to zero. This effect is stronger when $b^{(2)}$ is larger. This local increase occurs in the few demes beyond the point in space where adaptation is expected to fail (horizontal intercepts of dashed lines in fig. 3: here, genetic variance attains the maximum as shown in fig. 1). We discuss this effect further in the next section.

Decomposing a single optimal phenotype into two optimal phenotypes

We aimed at understanding whether a range-expanding population attains a larger (or smaller) range when a composite environmental gradient is decomposed into environmental selection acting on two traits as opposed to it acting on one trait only. To this end, we compared the model with a single composite adaptive trait (phenotype $z^{(c,i)}$) to the model with two orthogonal traits, and explored the same values of $b^{(2)}$ as in the previous section (fig. 4).

With a single trait, the range follows closely the theoretical expectations [Polechová and Barton, 2015]

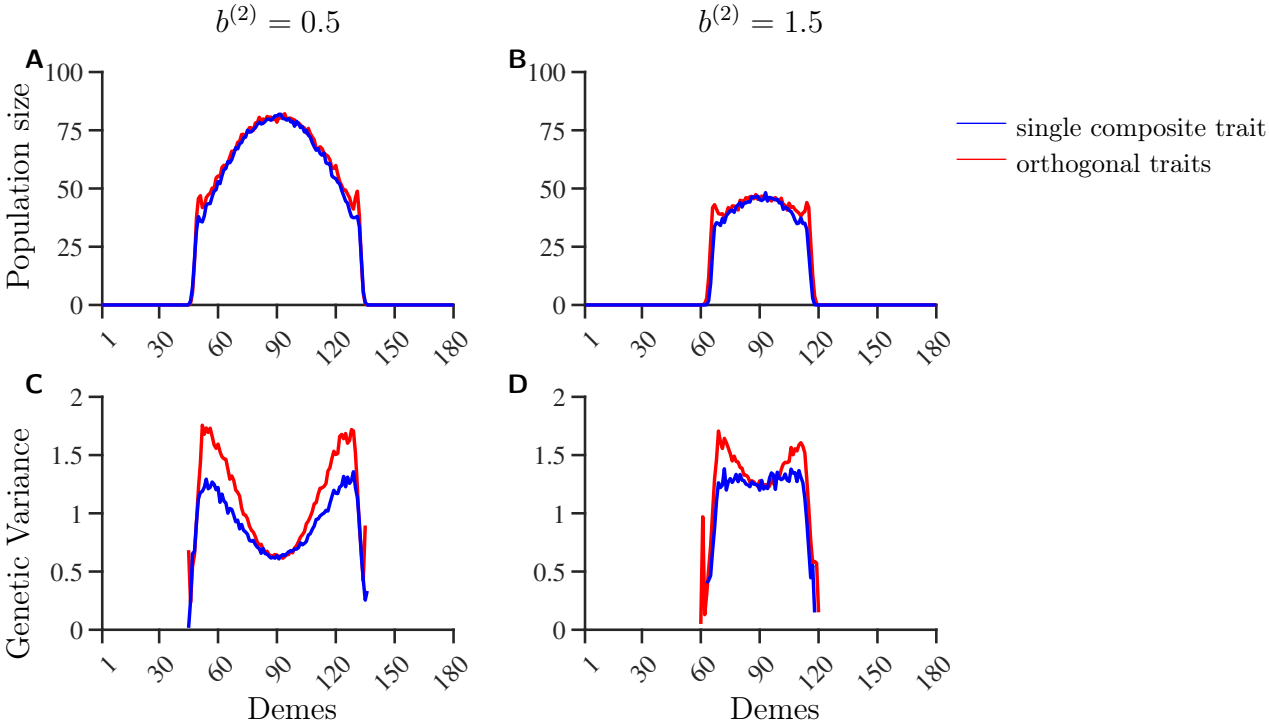

Figure 4: Comparison of population size and genetic variance between a single-trait model with single composite gradient $\theta^{(c,i)}$ (blue line), and two-trait model (red line). Measurements were taken before migration and after selection. Panels (A), (B): population size averaged over 50 independent realisations for different values of the steepness of the constant gradient, $b^{(2)} = 0.5$ (A) and $b^{(2)} = 1.5$ (B), as a function of deme position. Panels (C), (D): total genetic variance $v^{(\mathrm{tot},i)}$, defined for two traits as $v^{(\mathrm{tot},i)} = v^{(1,i)} + v^{(2,i)} + 2\mathrm{Cov}(z_l^{(1,i)}, z_l^{(2,i)})$, averaged over 50 independent realisations for different values of the steepness of the constant gradient, $b^{(2)} = 0.5$ (C) and $b^{(2)} = 1.5$ (D), as a function of deme position. Other parameters: $\alpha = 1/\sqrt{10}$, $V_s = 2$, $\sigma = 1$, $r_{\max} = 1$, $L = 654$, $K = 100$, and $\theta^{(1,i)}$, $\theta^{(2,i)}$ as given in Appendix A, (S1) and (S2) respectively.

with respect to the steepness of the gradient at the range margin (table 2), as well as the expected population size (fig. 4A, B). With two traits, by contrast, the realised range was up to 5 demes larger than with only one trait (table S1, Appendix A). At the same time, the composite steepness at the margins was $6 - 18\%$ larger in the two-trait model (table 2).

The small increase of population size as the margins is a feature of the two-trait model, but does not appear in the composite single-trait model. At the margins, the population was less maladapted (as measured by the population size) in the two-trait model than in the single composite trait model (fig. 4A, B). This was reflected in the mean population fitness, which was larger at the margins in the two-trait model than in the single-trait model (fig. S11, Appendix C).

We also compared the total variance in both models, defined as $v^{(\mathrm{tot},i)} = v^{(1,i)} + v^{(2,i)} + 2\mathrm{Cov}(z_l^{(1,i)}, z_l^{(2,i)})$. In the single-trait model, $\mathrm{Cov}(z_l^{(1,i)}, z_l^{(2,i)})$ is the variance due to linkage disequilibrium between pairs of loci that were assigned to the separate traits in the two-trait model (although in the single-trait model, all loci contribute to the same trait). The two-trait model exhibits more variance towards the margins than the composite single-trait model (fig. 4C,D). While part of this difference can be attributed to the covariance between traits (fig. S4, Appendix B), before migration this quantity is not large enough to explain all the difference (fig. S8, Appendix B). On the contrary, after migration, total genetic variance at the margins is the same in the composite single-trait model and the two-trait model (fig. S9). Interestingly, the after-migration covariance between the phenotypes of the traits in the two-trait model, as well as the after-migration covariance between the two phenotype components (underlain by the corresponding sets of loci) in the single-trait model, present significant proportions of total genetic variance attained after migration in the models (fig. S10). But, with two adaptive traits, the covariance does not explicitly affect individuals' fitness (eq. (1)). This suggests that with two adaptive traits the population can afford to build-up more genetic variance before migration (as observed in fig. 4) and still attain sufficient adaptation to persist locally.

steepness $b^{(2)}$	$b^{(1,m)} + b^{(2)}$ [mean (SD)]	
	two-trait model	single-trait model
$b^{(2)} = 0$	1.6 (0.3)	1.6 (0.3)
$b^{(2)} = 0.5$	1.7 (0.2)	1.6 (0.4)
$b^{(2)} = 1$	1.9 (0.2)	1.6 (0.3)
$b^{(2)} = 1.5$	1.9 (0.1)	1.6 (0.2)
single trait expectation [Polechová and Barton, 2015]		$b^{(1,m)} \approx 1.65$

Table 2: Maximal steepness at the margins of the realised range, indicating the critical steepness beyond which adaptation fails. We show the sum of both gradients $b^{(1,m)} + b^{(2)}$ at the realised margins (*i.e.* deme m, defined as the deme where $v^{(1,m)} + v^{(2,m)}$ is maximal; covariances were ignored here, as their relative contribution to the maximal variance was negligible) for the two-trait model and the composite single-trait model. Values were calculated by first determining where the maximum of the sum of adaptive variances is attained in each replicate, and measuring steepness of the composite gradient in that deme (on both sides), then averaging over the two to obtain an estimate for each replicate. The standard deviation is the uncorrected standard deviation (square root of the sample variance) over 50 replicates, each with two margins. The last row is the maximal steepness at which the population is expected to be able to adapt in the single steepening gradient model [Polechová and Barton, 2015].

Discussion

To expand over a habitat with a steepening environmental gradient and attain sufficient local adaptation, it is necessary that the genetic variance increases spatially: when the local variance cannot increase sufficiently, adaptation fails and range margins form [Polechová and Barton, 2015]. In the two-trait model, we showed that the formation of a range margin is determined by the combined effect of both gradients in the optimal phenotypes (figs. 1, 3), and that a range margin may form even when the steepening gradient is locally shallower than the constant gradient (fig. 2, table 2). In fact, in the scenario with the steepest constant gradient that we simulated ($b^{(2)} = 1.5$), the steepness of the steepening gradient at the margin was approximately 4 times smaller than the steepness of the constant gradient (fig. 2, table 2), and yet it had a fundamental role in the establishment of the range margins.

With two adaptive traits, the population size in equilibrium can be expressed in the same form and

parameters as in the single-trait model, upon using the sum of adaptive genetic variances (*i.e.* $v^{(\mathrm{sum},i)} = v^{(1,i)} + v^{(2)}$) in place of the genetic variance (eq. (3), also see Polechová and Barton [2015]). Interestingly, in our two-trait model, genetic variances for the traits evolve largely independently of each other, that is, the realised genetic variance for a given trait in the two-trait model agrees with the realised genetic variance in the model where only this trait is adaptive (figs. S12-S13, Appendix D). Because local genetic variance $v^{(j,i)}$ for adaptive trait j is expected to be proportional to the steepness $b^{(j,i)}$ of the gradient in the optimum [Barton, 2001], it follows that the local genetic variance governing the size in the two-trait model is proportional to the total (composite) gradient, *i.e.* $v^{(\mathrm{sum},i)} = (b^{(1,i)} + b^{(2)})\sigma\sqrt{V_s}$. This means that a population expanding over a larger composite environmental gradient, even if one of the two gradients is constant in space (but non-zero), will attain a smaller range.

In the second part of this study, we compared the range expansion of a population expanding over a single composite environmental gradient acting on a single adaptive trait, to the range expansion when the same composite environmental gradient is decomposed into selection acting on two separate traits. In the two-trait model, the covariance between traits generated by gene flow does not contribute to fitness explicitly (Appendix B, eq. S13), and the spatial evolution of genetic variance in each trait individually is more efficient than when the total environmental selection acts on a single trait alone (fig. 4C, D). In other words, when the adaptive response to an environmental gradient is decomposed into two traits, the population can harbour more genetic variance without incurring more maladaptation at the margins, thereby allowing for larger ranges.

This can be understood by comparing an individual's fitness reduction due to a given deviation of the individual's phenotype(s) from the optimum in the two models: we find that the reduction in the phenotype-dependent fitness component is smaller in the two-trait than in the single-trait model (Appendix B). As a consequence, the average phenotype-dependent fitness component realised after migration (and before selection) is larger in the two-trait model than in the single-trait model, particularly in areas where genetic variance is large (*i.e.* close to the margins; fig. S11C, D, Appendix D). This allows selection to be more efficient in the vicinity of range margins when it is decomposed to two adaptive traits, rather than one. Indeed, in the vicinity of the deme where adaptation fails in the single-trait model, the realised local population size is larger in the two-trait model (fig. 3), consistent with locally smaller maladaptation in this case. In turn, this allows the population to establish pockets (consisting of several demes) with locally well-adapted individuals, and expand beyond the range margins attained in the single-trait model. However, genetic variance in such pockets is typically small, and this precludes range expansion beyond the pockets. Selfing could strengthen this 'pocket' effect, but whether or not selfing is necessary to generate such pockets is an open question (recall also that selfing occurs in the single-trait model as well, but such pockets are absent).

Although empirical evidence supporting the steepening-gradient hypothesis exists [Johannesson and Andre, 2006, Johannesson et al., 2020], Kottler et al. [2021] showed that two key prediction of the steepening-gradient hypothesis, namely asymmetric gene flow and populations being more abundant in the center than in the margins, lack strong, general empirical support (see also Sagarin et al. [2006]). However, our simulations demonstrate that when the gradient in the optimum that changes linearly in space is large (large $b^{(2)}$), the population size at the center of the range is not much larger than the population size close to the margins, owing to the total gradient being mostly determined by the (steep) constant gradient (cyan line in fig. 3). By further increasing the steepness of the constant gradient (but not too much, to avoid rapid global extinction) and/or by adding further components of environmental selection and

respective adaptive traits, we expect that the concavity of the realised population size would decrease even further. This may explain the lack of strong empirical support for asymmetric gene flow and the decrease of population size from the center outwards in natural species' ranges. In addition, we found that the spatial patterns of the population size and fitness in the vicinity of range margins differ between the single-trait and the two-trait model. Adding such complexities and biological realism to the theoretical models (*e.g.* considering more than two traits and trade-offs) is a promising way forward to understand the evolutionary causes and consequences of limits to species' ranges.

Throughout this study we assumed that fitness was governed by two adaptive traits. Although many different environmental variables can be involved in shaping the spatial patterns in optimal phenotypes of adaptive traits, one possibility is that the two adaptive traits are under selection with respect to two different environmental variables, and that the spatial gradient in the optimal phenotype for each trait is correlated to the spatial gradient in the corresponding environmental variable. In this case, the mean local phenotype for a given adaptive trait will be a linear function of the local value of the corresponding environmental variable. This is an ideal case for environmental association analyses, where a linear relationship between the adaptive trait value and the value of the 'causal' environmental variable is typically assumed (see *e.g.* Benito Garzón et al. [2019]). The results of environmental association analyses can then be used to guide management and conservation actions. For example, "assisted migration" can be implemented to achieve an estimated "trait shift" needed to avoid severe maladaptation (and hence extinction) under future environmental conditions, or to simply assist the movement of a population towards new areas where the population would suffer from a smaller (estimated) risk of maladaptation (see *e.g.* Rellstab et al. [2021]). Notably, our results show that situations exist such that a steepening gradient in the optimum of an adaptive trait can be very shallow (almost flat) throughout the entire contemporary range (but not necessarily outside of the realised range), and yet it can have a fundamental role in the establishment of range margins. In such situations, both the causal steepening environmental gradient and the adaptive trait under the corresponding environmental selection can be missed or overlooked (due to potential statistical power issues associated with a small steepness of the gradient), and this can have serious negative consequences on assisted migration and similar management and conservation actions.

While we simulated an expanding population with two adaptive traits, mathematical analysis suggests that our findings can be extended to situations with more adaptive traits (Appendix B); the formation of range margins will again depend on the net genetic load stemming from all adaptive traits involved. Landscape [Manel and Holderegger, 2013] and seascape genomic studies [Dayan, 2020] suggest that many environmental variables may be involved in shaping spatio-temporal population dynamics. If all the underlying environmental variables had constant gradients, this would correspond to a scenario in which a population evolved along one composite constant gradient. As long as the composite environmental condition changes linearly across the habitat, a population is expected to adapt indefinitely – provided that it does not encounter "trivial" margins (*sensu* Eriksson and Rafajlović [2022]). However, if any of the gradients steepens at some point in space, this can potentially lead to the formation of a range margin. When the total gradient is steeper (*i.e.* there are more components of environmental selection that may or may not act on separate traits), the change needed in only one of the optimal phenotypes to potentially form a range margin becomes smaller. This reinforces the importance of the steepening-gradient hypothesis: in a scenario involving multiple environmental gradients acting on two or more adaptive traits, a small change in the local steepness of the gradient of only one optimal phenotype is enough to cause the establishment of an abrupt range margin.

In our model, we made several simplifying assumptions, such as free recombination, and absence of plasticity. When recombination between loci is reduced, the steepening-gradient hypothesis is still valid [Eriksson and Rafajlović, 2021]. Reduced recombination between adaptive loci may (at least transiently) mitigate the effects of migration load [Eriksson and Rafajlović, 2021]. Similarly, we may expect transiently larger range extents in our model if the loci of one or both of the traits recombined less frequently. However, it is an open question how the recombination rate between loci underlying separate adaptive traits would impact on the rate of the range expansion and the establishment of range margins.

When it comes to plasticity, theoretical analysis showed that, while expanding along a steepening gradient, if plasticity comes at no, or very low cost, the formation of a range limit may be suppressed [Eriksson and Rafajlović, 2022]. However, if plasticity is sufficiently costly, it can increase the range extent, but not indefinitely [Eriksson and Rafajlović, 2022]. In such cases the steepening-gradient hypothesis is still valid. While empirical evidence for plasticity costs is sparse [Auld et al., 2010, Murren et al., 2015], it has been argued that the presence of range margins along smooth gradients (not mediated by other factors) is indirect evidence that costs and/or limits to plasticity exist [DeWitt et al., 1998].

In sum, our study shows that, in the absence of any obvious geographical barriers, adaptation involving multiple traits, of which at least one has optimal phenotype with a steepening gradient, is sufficient to obtain a finite range. When the number of environmental gradients involved is larger, the required change in just one of the gradients, that is sufficient to cause range margins, is smaller. Such shallow gradients can be easily overlooked in field studies. We further showed that if the selection pressure is decomposed between two traits, the population can withstand higher genetic load, which in turns means that, before adaptation fails abruptly, populations can evolve more genetic variance and expand further when selection is decomposed between two adaptive traits, than when it acts on a single adaptive trait. Because of this, the steepening-gradient hypothesis may be consistent with the evolution of novel traits that might help a population to expand into a new territory, an observation that has been highlighted in a recent study [Santos et al., 2017]. In general, climate change has recently been linked to rapid trait evolution (*e.g.* Mackin et al. [2021]).

In natural populations, there are likely many adaptive traits, and we show here that if at least one of them has even a slightly steepening gradient in the optimal phenotype, it can be detrimental to the possibility of local adaptation, potentially causing the establishment of sharp range margins. We argue that our results support the steepening-gradient hypothesis as an innate explanation of species' range limits (when geographical barriers are absent), without the need for extensively steepening gradients in any individual trait optimum.

Acknowledgments

We thank Roger K. Butlin for discussions on the topic and insightful comments on earlier versions of the manuscript, and members of the Linnaeus Centre for Marine Evolutionary Biology (CeMEB, https://www.gu.se/en/cemeb-marine-evolutionary-biology) for feedback and discussions on this topic. This work was funded by the Swedish Research Council Formas to KJ and MR (grant number 2019-00882). MR was also supported by a grant from Vetenskapsrådet (to MR; grant number 2021-05243), Hasselblad Foundation Grant for Female Scientists (to MR), and by the European Research Council (through CeMEB). Simulations were enabled by resources provided by the Swedish National Infrastructure for Computing (SNIC) at the Uppsala Multidisciplinary Center for Advanced Computational Science (UPPMAX, project SNIC 2021-22-286), and at the High Performance Computing Center North

(HPC2N, project SNIC 2021-5-501), both partially funded by the Swedish Research Council through grant agreement no. 2018-05973.

Authors contributions

MR conceived the study. ME and MR designed the simulations with input from MT. ME wrote the code of the simulations. MT ran simulations. MT analyzed simulation results with input from ME and MR. MT did the theoretical calculations with input and feedback from ME and MR. MT, ME and MR interpreted the results with input from KJ. MT wrote the first draft of the manuscript. All the authors revised and edited the manuscript. MR supervised the study.

Methods

Simulations

We performed individual-based simulations to investigate how the presence of two adaptive traits impacts on the process of range expansion and on the establishment of range margins. To this end, we extended the simulation framework used in Eriksson and Rafajlović [2021, 2022]. Simulations were custom-made and implemented in Matlab. The code will be deposited on Dryad upon acceptance of the manuscript.

Similarly to Eriksson and Rafajlović [2021, 2022], we modelled the habitat as a unidimensional lattice of $M = 180$ demes of equal size. We measured the distance along the habitat in units of the distance between consecutive demes (thus, the distance between each pair of consecutive demes was set to 1 in the model). Each deme had a carrying capacity of $K = 100$ diploid, monoecious individuals with non-overlapping generations. We assumed that there were two polygenic traits under selection (*i.e.* adaptive traits) $\mathcal{Z}^{(1)}$ and $\mathcal{Z}^{(2)}$. The optimal phenotype $\theta^{(1,i)}$ for trait $\mathcal{Z}^{(1)}$ was given by a cubic polynomial of $i \in \{1, 2, \ldots, M\}$ with an inflection point in the centre of the habitat (that is, the gradient in the optimal phenotype was gradually steepening, eq. S1, Appendix A; figure 2). The optimal phenotype for trait $\mathcal{Z}^{(2)}$ was assumed to change linearly in space, with slope $b^{(2)}$ (eq. S2, Appendix A; figure 2). With our parametrisation, the habitat centre was symmetric around demes 90 and 91, with $-\theta^{(2,90)} = \theta^{(2,91)} = b^{(2)}/2$.

Each trait was underlain by $L = 654$ biallelic loci contributing additively to the traits with possible effect sizes of $\pm\alpha/2$. We used $\alpha = 1/\sqrt{10}$ (values were selected within the range of parameters explored in Polechová and Barton [2015] and used *e.g.* by Eriksson and Rafajlović [2022]). The number of loci was selected in such a way that the maximal value of the optimal phenotype with the steepening gradient ($-\theta^{(1,1)} = \theta^{(1,M)} = 206.7$) was the equal to the maximal phenotype that an individual could possibly attain with the parameters we chose, *i.e.* $L\alpha$. For all parametrisations of the linear optimal phenotype (see later in this section), the absolute maximal optimal phenotype in the habitat $\theta^{(2,M)}$ was smaller than the maximal optimal phenotype $\theta^{(1,M)}$ for the trait with a steepening optimal phenotype.

At each generation τ, for each deme i, the phenotype $z^{(j,i)}_{\tau,l}$ of individual $l \in \{1, 2, \ldots, N^{(i)}_\tau\}$ (with $N^{(i)}_\tau$ denoting the population size in deme i at generation τ), for trait $j \in \{1, 2\}$, was equal to the sum of all allelic effect sizes at the L loci underlying that trait. The growth rate $r^{(i)}_{\tau,l}$ of individual l in deme i, in generation τ was determined by its phenotypes $z^{(1,i)}_{\tau,l}$ and $z^{(2,i)}_{\tau,l}$ according to eq. (1) in the main text. The first term in eq. (1) stands for density regulation around the carrying capacity K. In this term, $r_{\max}$ is the maximal intrinsic growth rate of the population, and we set it to $r_{\max} = 1$ throughout. The second and the third term are the contributions due to selection acting on the first and second trait, respectively,

in line with Fisher's geometric model involving two orthogonal traits [Fisher, 1930]. Here, V_s is the width of stabilizing selection.

To understand how an additional selection component in the form of a constant gradient may modify the establishment of range margins, we first compared this model with two adaptive traits with the model involving only one adaptive trait with the steepening gradient in $\theta^{(1,i)}$ (upon setting $V_s \to \infty$ for the second trait, making it a neutrally evolving trait). Thereafter, we aimed at understanding if a population is more or less successful in expanding its range when a composite environmental gradient is decomposed into environmental selection acting on two traits as opposed to it acting on one trait only. To achieve this, we compared our two-trait model with a single-trait model where the phenotype was $z_{\tau,l}^{(c,i)} = z_{\tau,l}^{(1,i)} + z_{\tau,l}^{(2,i)}$, and a composite optimal phenotype $\theta^{(c,i)} = \theta^{(1,i)} + \theta^{(2,i)}$, and the growth rate $r_{\tau,l}^{(c,i)}$ as given in eq. (2).

The life-cycle was modelled as follows: selection, recombination, mutation of gametes, fertilization and migration. At each generation τ, the number of gametes that individual l in deme i contributed to the next generation was assumed to be a random number sampled from a Poisson distribution with mean $2 \exp r_{\tau,l}^{(i)}$ (same with $r_{\tau,l}^{(c,i)}$ in the composite single-trait model). For each gamete, recombination occurred independently, and we assumed that all loci recombine freely. After recombination, mutation occurred with probability $\mu = 10^{-6}$ per generation, individual and allele, and it was assumed to be a symmetric and reversible process between the two possible alleles at each locus. Pairs of haploid gametes from the same deme were then chosen uniformly at random to form new zygotes (as such, selfing was possible by chance). After reproduction, parents were removed from the population, and the newly formed zygotes dispersed according to a discretised Gaussian function with mean 0 and standard deviation $\sigma = 1$ (as in [Eriksson and Rafajlović, 2022]). After dispersal, the zygotes were treated as adults, and the cycle entered the next generation.

Each simulation was initialised with a population occupying $M/5 = 36$ demes in the center of the habitat, with all other demes empty. The starting mean phenotypes in each deme were assumed to match the optimal phenotypes (of each trait) in that deme. To realize the initial mean phenotype, $\lceil L/5 \rceil$ loci (with $\lceil x \rceil$ denoting the smallest integer larger than or equal to x) were selected at random and assigned allele frequencies according to the expected allele frequency clines [Barton, 2001] for a model with a single trait. The allele frequencies at the remaining loci were chosen in such a way to not change the mean phenotypes in each deme [Eriksson and Rafajlović, 2021].

We ran each simulation for $100,000$ generations, and we performed 50 replicates for each set of parameter values. We measured population size, mean phenotype per deme, genetic variance of each trait, as well as covariance between the traits, and spatial patterns of allele frequencies. All measures were done both before and after migration in the life-cycle. We allowed the population to expand from the center of the habitat, and compared the realised range extent of a population with two adaptive traits to the range that would be reached when only the trait with the steepening gradient in the optimum is *adaptive* (*i.e.* upon setting the second trait to a neutrally evolving trait; this is because in the presence of solely a constant gradient in the optimal phenotype, the population is expected to either occupy the entire available habitat, or experience global extinction). We tested four different slopes $b^{(2)}$ for the constant gradient, *i.e.* $b^{(2)} \in \{0, 0.5, 1.0, 1.5\}$. These values were chosen in such a way that in the absence of any other gradients, the range would extend until the end of the habitat [Barton, 2001, Polechová and Barton, 2015]. In the model with two orthogonal traits, the maximal value of $b^{(2)}$ that allows a population to attain a finite (non-zero) range was $b^{(2)} \approx 2$ (simulations with $b^{(2)} = 2$ and larger, not shown, led to either very small populations adapted only in a few demes in the center, or to total collapse over the

whole range).

While many of the quantities described in this section (*e.g.* $z_{\tau,l}^{(j,i)}$, $N_\tau^{(i)}$, *etc.*) evolve over time τ and space i, at the end of each simulation the expanding population will have reached a state of quasi-equilibrium (typically, for the parameter sets we tested, this state was reached after 10-20,000 generations; figure S1, Appendix A). This state is not a proper equilibrium, because global extinction will ultimately occur, *albeit* this is expected after much longer times than those simulated here [Eriksson et al., 2013]. Thus, the quasi-equilibrium is arguably long lasting (in terms of timescales that are of biological interest), and it is the properties of the quasi-equilibrium that we are interested in. For simplicity, however, we refer to this state as *equilibrium* throughout. Furthermore, we also note that we omit the generation index τ when denoting quantities in equilibrium. The results obtained under the model described are shown and discussed in the main text, as well as in the Appendices.

References

J. R. Auld, A. A. Agrawal, and R. A. Relyea. Re-evaluating the costs and limits of adaptive phenotypic plasticity. *Proceedings of the Royal Society B: Biological Sciences*, 277(1681):503–511, 2010.

N. H. Barton. Adaptation at the edge of a species' range. In J. Silvertown and J. Antonovics, editors, *Integrating ecology and evolution in a spatial context*, volume 14, pages 365–392. Blackwell, Oxford, 2001.

M. Benito Garzón, T. M. Robson, and A. Hampe. δtrait sdms: species distribution models that account for local adaptation and phenotypic plasticity. *New Phytologist*, 222(4):1757–1765, 2019.

J. R. Bridle and T. H. Vines. Limits to evolution at range margins: when and why does adaptation fail? *Trends in ecology & evolution*, 22(3):140–147, 2007.

T. J. Case, R. D. Holt, M. A. McPeek, and T. H. Keitt. The community context of species' borders: ecological and evolutionary perspectives. *Oikos*, 108(1):28–46, 2005.

D. I. Dayan. Clinal adaptation in the marine environment. In M. F. Oleksiak and O. P. Rajora, editors, *Population genomics: marine organisms*, pages 221–247. Springer Nature Switzerland AG, 2020.

T. J. DeWitt, A. Sih, and D. S. Wilson. Costs and limits of phenotypic plasticity. *Trends in ecology & evolution*, 13(2):77–81, 1998.

A. Eriksson, F. Elías-Wolff, and B. Mehlig. Metapopulation dynamics on the brink of extinction. *Theoretical population biology*, 83:101–122, 2013.

M. Eriksson and M. Rafajlović. The effect of the recombination rate between adaptive loci on the capacity of a population to expand its range. *The American Naturalist*, 4 2021. ISSN 0003-0147. doi: 10.1086/713669.

M. Eriksson and M. Rafajlović. The role of phenotypic plasticity in the establishment of range margins. *Philosophical Transactions of the Royal Society B*, 377(1846):20210012, 2022.

R. A. Fisher. *The genetical theory of natural selection*. Clarendon Press, Oxford, 1930.

R. Gomulkiewicz, R. D. Holt, and M. Barfield. The effects of density dependence and immigration on local adaptation and niche evolution in a black-hole sink environment. *Theoretical population biology*, 55(3):283–296, 1999.

J. B. S. Haldane. The relation between density regulation and natural selection. *Proceedings of the Royal Society of London. Series B-Biological Sciences*, 145(920):306–308, 1956.

R. D. Holt. On the evolutionary ecology of species' ranges. *Evolutionary ecology research*, 5(2):159–178, 2003.

K. Johannesson and C. Andre. Invited review: Life on the margin: genetic isolation and diversity loss in a peripheral marine ecosystem, the baltic sea. *Molecular Ecology*, 15(8):2013–2029, 2006.

K. Johannesson, A. Le Moan, S. Perini, and C. André. A darwinian laboratory of multiple contact zones. *Trends in Ecology & Evolution*, 2020.

M. Kirkpatrick and N. H. Barton. Evolution of a species' range. *The American Naturalist*, 150:1–23, 1997.

E. J. Kottler, E. E. Dickman, J. P. Sexton, N. C. Emery, and S. J. Franks. Draining the swamping hypothesis: Little evidence that gene flow reduces fitness at range edges. *Trends in Ecology and Evolution*, 2021. ISSN 01695347. doi: 10.1016/j.tree.2021.02.004.

R. H. MacArthur. *Geographical Ecology.* Harper & Row, New York, USA, 1963.

C. R. Mackin, J. F. Peña, M. A. Blanco, N. J. Balfour, and M. C. Castellanos. Rapid evolution of a floral trait following acquisition of novel pollinators. *Journal of Ecology*, 109(5):2234–2246, 2021.

S. Manel and R. Holderegger. Ten years of landscape genetics. *Trends in ecology & evolution*, 28(10): 614–621, 2013.

E. Mayr. *Animal species and evolution.* Harvard University Press, 1963.

C. J. Murren, J. R. Auld, H. Callahan, C. K. Ghalambor, C. A. Handelsman, M. A. Heskel, J. Kingsolver, H. J. Maclean, J. Masel, H. Maughan, et al. Constraints on the evolution of phenotypic plasticity: limits and costs of phenotype and plasticity. *Heredity*, 115(4):293–301, 2015.

J. R. Peck, J. M. Yearsley, and D. Waxman. Explaining the geographic distributions of sexual and asexual populations. *Nature*, 391(6670):889–892, 1998.

J. Polechová. Is the sky the limit? on the expansion threshold of a species' range. *PLoS biology*, 16(6): e2005372, 2018.

J. Polechová and N. H. Barton. Limits to adaptation along environmental gradients. *Proceedings of the National Academy of Sciences*, 112(20):6401–6406, 2015.

C. Rellstab, B. Dauphin, and M. Exposito-Alonso. Prospects and limitations of genomic offset in conservation management. *Evolutionary Applications*, 14(5):1202–1212, 2021.

R. D. Sagarin, S. D. Gaines, and B. Gaylord. Moving beyond assumptions to understand abundance distributions across the ranges of species. *Trends in ecology & evolution*, 21(9):524–530, 2006.

M. E. Santos, A. Le Bouquin, A. J. Crumière, and A. Khila. Taxon-restricted genes at the origin of a novel trait allowing access to a new environment. *Science*, 358(6361):386–390, 2017.